

# USE OF AN INR-STYLE BUNCH-LENGTH DETECTOR IN THE FERMILAB LINAC

Elliott S. McCrory and Charles W. Schmidt  
 Fermi National Accelerator Laboratory\*  
 Batavia, IL 60510, USA

A. V. Feschenko  
 Institute for Nuclear Research of the Russian Academy of Sciences  
 Moscow, 117312, Russia

## ABSTRACT

A device to accurately measure the phase extent of a linac beam is being developed for use in the Fermilab 400 MeV Linac Upgrade [1]. Prototypes have been and are being tested. We have attempted to improve the original design from the Institute for Nuclear Research in Moscow (INR) [2] to increase the resolution for adequate operation at 805 MHz. The device incorporating a new arrangement of lens and deflector, reported previously [3], cannot achieve the desired resolution.

This paper describes the operation and the strengths and weaknesses of the three types of bunch-length detectors (BLDs) and the measurements made at this time. The differences among these devices is delineated by the relative position of the rf deflector and the electrostatic einzel lens, as follows:

INR	Lens before deflector	Figure 1
Fermilab	Lens after deflector; H- beam	Figure 2
FNAL/INR	Lens and deflector combined	Figure 3

To satisfy the goals of commissioning the new linac, a resolution of about 5 picoseconds ( $1^\circ$  at 805 MHz) is desired.

## PRINCIPLE OF OPERATION

Referring to the reference [4] and to Figure 1, an INR BLD works as follows. The primary ion beam impinges on a retractable wire target, 1, which is at negative high voltage,  $V \approx -10\text{kV}$ , wire  $\varnothing = 125 \mu\text{m}$ . The passage of the beam through the wire causes secondary electrons to be liberated from the atoms in the wire. Free secondary electrons near the surface migrate out of the wire and are accelerated radially away from it by the voltage,  $V$ , to the collimator, 2. An electrostatic einzel lens, 3, then focuses the electrons onto the slit at the far end of the detector, 5. Along the way, the electrons are deflected by the rf deflector, 4, which oscillates with a voltage equal to  $U(t) = A\cos(\omega t + \phi)$ , where  $\omega$  is equal to a multiple of the Linac bunching frequency and  $\phi$  is a controllable phase angle. The transit time through the deflector is approximately  $\pi$ . For some initial angle  $\phi$ , the electrons will pass through the slit, 5, and enter the electron detector, 6. This detector can be a faraday cup or an electron multiplier tube. Because the temporal distribution of the

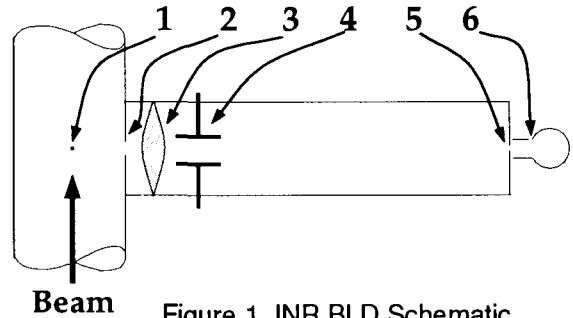


Figure 1, INR BLD Schematic  
 electron beam on the plane of the collector slit is determined by the deflector, not by the electron detector, the bandwidth of the electron detector is largely irrelevant. It can, in fact, be an integrator. The intensity of the signal on 6 as a function of the phase angle  $\phi$  is equivalent to the density of the primary ion beam as a function of the bunching phase angle.

The operation of the other types of BLDs is similar. In the Fermilab device, a higher gradient is necessary in order to compensate for the focussing of the lens. The electron beam line is tuned off-line by using thermionically emitted electrons emitted from the wire when it is heated by a current (for us, 1 to 2 A at 60Hz).

## RESOLUTION OF THE DETECTORS

Several significant factors determine the resolution of these devices. Four major effects are considered here

The first factor is the time necessary for the secondary electrons to be ejected from the wire. This time has been measured [5] at  $<6 \text{ ps}$ , or  $1.74^\circ$  at the bunching frequency of the Fermilab 400 MeV Linac, 805 MHz.

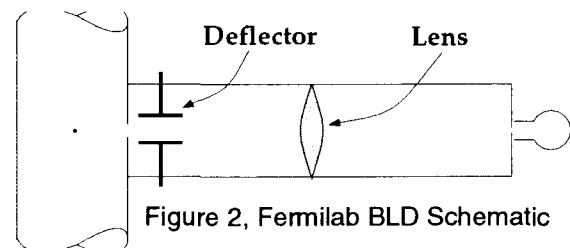


Figure 2, Fermilab BLD Schematic

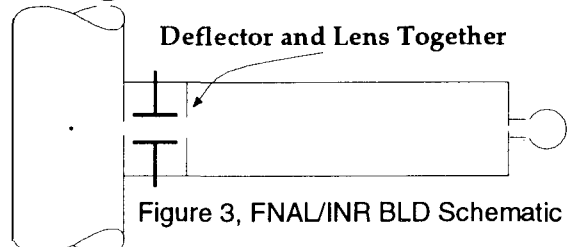


Figure 3, FNAL/INR BLD Schematic

\* Fermilab is operated by the Universities Research Association under contract to the US Department of Energy.

The second factor is the emittance of the secondary electron beam. A velocity spread arises from the thermal velocities of the secondary electrons before they are ejected from the wire. The resolution here is proportional to  $d/V^2$  where  $d$  is the drift from the target to the deflector and  $V$  is the voltage on the target. It is possible to reduce this effect to about 1 ps by shortening the drift distance and by using 10 kV on the target. The transverse emittance has essentially no effect on the resolution.

The third effect is the path-length differences among the electrons and is determined by the optics of the electron beamline. Those electrons which travel away from the center line of the detector take longer to reach the deflector than the electrons which travel on the axis of the device. This effect is likewise proportional to the drift from the target to the deflector. Also, if the lens is farther away from the target (decreasing the magnification of the image and reducing the spread of the beam), this effect is also reduced. Again, using a higher voltage and a shorter drift, this effect reduces the resolution by only about about 0.5 ps.

The fourth effect is the strength of the rf deflector. A stronger deflection, to first order, will increase the resolution. For a deflection which is too large, part of the electron beam hits the deflecting plates for any  $\phi$ . Also, the fringing fields become more important. For the INR detector, a gradient of about 100 V/cm is optimum and good resolution is obtained (6 ps, or  $0.4^\circ$  at 198 MHz). For the Fermilab-type detector, it was thought that 5000 V/cm would be necessary to increase the resolution to below 5 ps, or  $1^\circ$  at 805 MHz.

A summary of these effects is presented in Table 1. Note that the INR detector was designed for a bunching frequency of 198 MHz with the deflector running at 594 MHz, whereas the other two are for 805 MHz. The total resolution for the INR detector is measured; for the other two, it is estimated.

Table 1.

Resolution of the Various BLDs

	INR	Fermilab	INR/FNAL
1	<6 ps	<6 ps	<6 ps
2	3.0	1.0	1.0
3	1.5	0.5	0.5
4	5.5	30?	6.0
Total	14 ps ( $1^\circ$ @ 198 MHz)	30 ps? ( $6^\circ?$ @ 805 MHz)	6 to 10 ps ( $1^\circ$ to $1.8^\circ$ )

Non-linear effects (space charge, lens aberrations) are not directly considered here. It is felt that these effect do not contribute significantly to the resolution of the device.

DEVELOPMENT OF THE FERMILAB DETECTOR

It was decided we would build a Fermilab-type detector for prototyping at 200 MeV. The device (Figure 2)

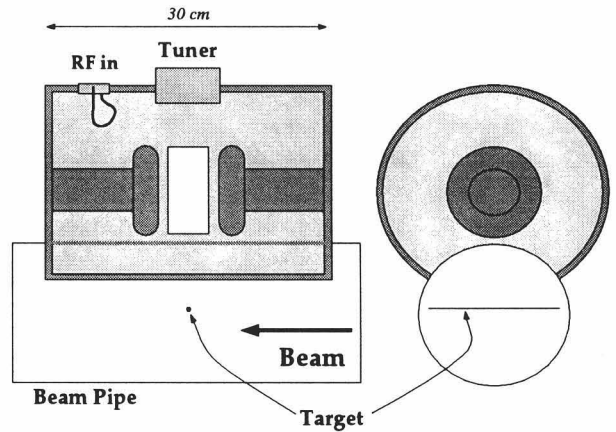


Figure 4, Schematic of the Fermilab Deflector

requires substantial power in the rf deflector. A suitable deflector has been fabricated, shown in Figure 4. We have applied 200 W to this cavity for a gradient of 5000 V/cm across its 3 cm gap. The interior of the deflector was coated with a thin (150 Angstrom) layer of titanium nitride to increase the limit for multipactoring.

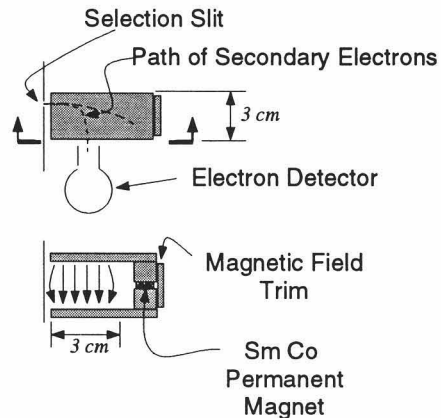


Figure 5, Selection Magnet

In order to reject the primary electrons scattered off the wire from our H- beam, it is necessary to install a permanent-magnet deflector (Figure 5) between the selection slit and the electron detector. The energy of the scattered electrons which would pass into our detector is several hundred keV, so rejecting these electrons is

easy. The permanent magnet used in this deflector is a samarium-cobalt magnet with a surface field of approximately 8000 Gauss. The field in the bending region has been trimmed to a value of about 133 Gauss, which corresponds to  $\rho=2.54$  cm for 10 keV electrons.

We have discovered two debilitating problems with this style of detector. (1) The electrons from the secondary electron beam will induce multipactoring at a power level no greater than 700 V/cm for our 3 cm gap. That threshold is reduced if electrons hit the inside of the rf chamber. This means we cannot achieve adequate gradient in the cavity to produce a satisfactory resolution. (2) The trajectory which passes through the first and the last collimator slits (and through the rf deflector) does not pass through the axis of the einzel lens. Thus, the einzel lens must have a relatively large aperture, larger than one would expect for an aberration-free lens. Moreover, this trajectory also exits from the rf deflector considerably off axis which may induce multipactoring.

We will not pursue this design further.

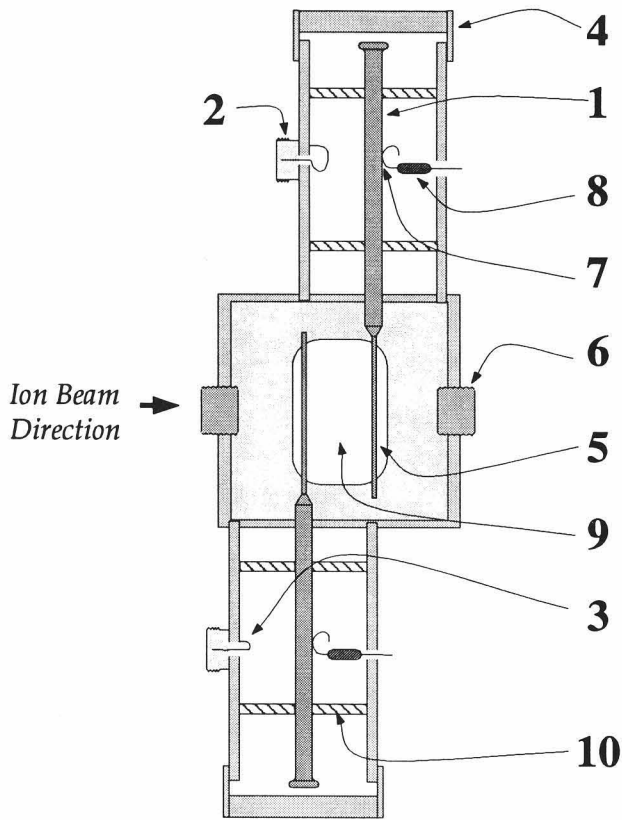


Figure 6, Deflector Schematic for FNAL/INR BLD

### THE FNAL/INR DETECTOR

A BLD with the best features of the other two has been developed. It combines the deflector and the einzel lens into a single unit. This arrangement has several benefits. It allows the deflector to be placed very close to the target, as in the Fermilab detector. Also, since the rf deflector plates have a negative DC potential applied to them for the lens, multipactoring should not occur.

The design of the deflector/lens is as follows (refer to Figure 6): Each of the two arms of the deflector form a resonant coaxial cavity, 1; the length of each arm is  $\lambda/2$  at our frequency of 805 MHz. One coupling loop provides the input rf power, 2, and the other loop provides the readback, 3. The resonant frequency of the two arms of the deflector is tuned by adjusting the end-caps, 4, and by trimming the size of the deflector plates, 5. Small slug tuners, 6, provide the final trimming to the desired resonant frequency.

The DC voltage for the lens is applied near the point of zero rf field along the center conductor of the coaxial arms, 7, at the  $\lambda/4$  point of each resonator through a 1 M $\Omega$  resistor, 8. Secondary electrons pass through the input slit and are deflected and focussed in the central region of the deflector, 9, and exit through the rear of the rf chamber. The exit aperture is large enough not to intercept any beam. The arms are supported by nylon rings, 10. The equivalent impedance  $R_{eq} = U_{max}^2/2P$  is measured to be 90 000  $\Omega$ , where  $U_{max}$  is the maximum rf voltage between the deflector plates and P is the

dissipated power.

The optimum deflecting gradient for this deflector has been estimated by computer simulation. The electric field in the deflector is calculated as a superposition of the electrostatic focusing field and the rf deflecting field using a quasi-static approximation. The field distribution is considered to be flat. The distribution of the electrostatic fields in the deflector chamber is taken to be the same as for a coaxial line and has been calculated analytically.

A delta-function incident ion beam is assumed and the size of the secondary electron image on the final selection slit is calculated. The resolution here is defined to be

$$\Delta\Phi = 2\sigma_e/X_{max},$$

where  $\sigma_e$  is the size of the electron beam at the detector slit and  $X_{max}$  is the maximum deflection on the plane of the detector slit caused by the rf deflector. 200 electrons are used in the simulation for the calculation of each point. The results are presented in Figure 7. It is interesting to note that the increase in the size of the electron beam is approximately cancelled for by the increasing amplitude of its deflection.

The deflector has been tested in vacuum. To obtain  $U_{max}=1000$  V, 5.6 W of rf power is required.

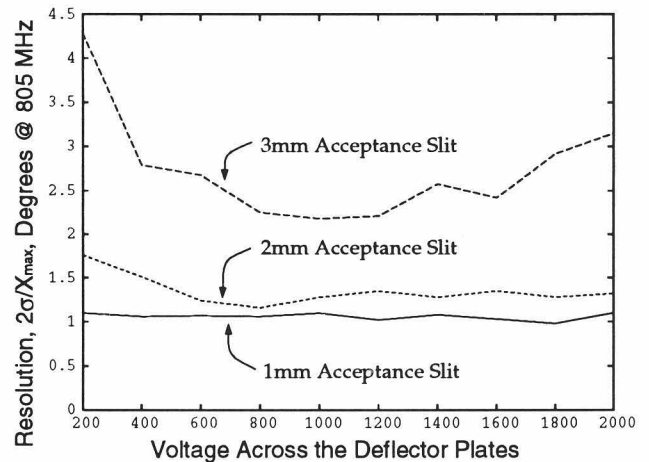


Figure 7, FNAL/INR BLD Resolution for various input collimators.

### REFERENCES

- [1] Robert J. Noble, "The 400 MeV Linac Upgrade at Fermilab," this conference, TH1-01.
- [2] A.V. Feschenko and P.N. Ostroumov, "Bunch Shape Measuring Techniques and its Application for an Ion Linac Tuning," 1986 Linac Conference Proceedings, SLAC, pp 323-327.
- [3] Elliott S. McCrory, Glenn Lee and Robert C. Webber, "Diagnostics for the 400 MeV FNAL Linac," 1990 Linac Conference Proceedings, Albuquerque, pp 456-458.
- [4] Elliott McCrory, "Design Considerations for a Bunch Length Monitor at the Fermilab Linac," FNAL Linac Upgrade Document number 161.
- [5] *Secondary Emission*, by Bronstein and Fraiman, pp 319-326; 1968, Nauka Publishing, Moscow, in Russian.